

Characterization and application in XRF of HfO_2-coated glass monocapillary based on atomic layer deposition

Yan-Li Li(李艳丽), Ya-Bing Wang(王亚冰), Wei-Er Lu(卢维尔), Xiang-Dong Kong(孔祥东), Li Han(韩立), Hui-Bin Zhao(赵慧斌)

Citation: Chin. Phys. B, 2021, 30 (**5**): 050703. DOI: 10.1088/1674-1056/abcfa2
Journal homepage: http://cpb.iphy.ac.cn; http://iopscience.iop.org/cpb

What follows is a list of articles you may be interested in

Property of slice square polycapillary x-ray optics

Shi-Qi Peng(彭诗棋), Zhi-Guo Liu(刘志国), Tian-Xi Sun(孙天希), Kai Wang(王锴), Long-Tao Yi(易龙涛), Kui Yang(杨魁), Man Chen(陈曼), Jin-Bang Wang(王金榜)

Chin. Phys. B, 2016, 25 (**2**): 024102. DOI: 10.1088/1674-1056/25/2/024102

Polycapillary X-ray lens for secondary focusing Beijing synchrotron radiation source

Li Yu-De, Lin Xiao-Yan, Liu Shi-Gang, He Jin-Long, Guo Fei, Sun Tian-Xi, Liu Peng

Chin. Phys. B, 2013, 22 (**4**): 044103. DOI: 10.1088/1674-1056/22/4/044103

Measurement of inner surface roughness of capillary by an x-ray reflectivity method

Li Yu-De, Lin Xiao-Yan, Tan Zhi-Yuan, Sun Tian-Xi, Liu Zhi-Guo

Chin. Phys. B, 2011, 20 (**4**): 040702. DOI: 10.1088/1674-1056/20/4/040702

Characterization and application in XRF of HfO_2-coated glass monocapillary based on atomic layer deposition*

Yan-Li Li(李艳丽)[1,†], Ya-Bing Wang(王亚冰)[2,†], Wei-Er Lu(卢维尔)[3], Xiang-Dong Kong(孔祥东)[1,4,‡], Li Han(韩立)[1,4], and Hui-Bin Zhao(赵慧斌)[1]

[1] *Institute of Electrical Engineering, Chinese Academy of Sciences, Beijing* 100190, *China*
[2] *College of Nuclear Science and Technology, Beijing Normal University, Beijing* 100875, *China*
[3] *Institute of Microelectronics, Chinese Academy of Sciences, Beijing* 100029, *China*
[4] *University of Chinese Academy of Sciences, Beijing* 100049, *China*

(Received 23 September 2020; revised manuscript received 4 November 2020; accepted manuscript online 2 December 2020)

Coating a glass monocapillary x-ray optics with high-density film is a promising way to improve transmission characteristics. For a long time, it has been a challenge to coat a high-density film in the inside of monocapillary with an extremely high length-to-diameter ratio. In this work, HfO_2 film is deposited on the inner wall of a tapered glass monocapillary with length 9.9 cm, entrance diameter 596.4 μm, and exit diameter 402.3 μm by atomic layer deposition. The coated and uncoated monocapillaries are studied by the transmission process of x-rays with energy from 5 keV to 100 keV and the x-ray fluorescence (XRF) spectra of a Mo sample are detected. Improved transmission characteristics have been obtained for the HfO_2-coated monocapillary. The energy upper limit of focused x-rays increases from 18.1 keV to 33.0 keV and the 'penetration halo' is suppressed to some extent. The XRF spectrum presents two stronger peaks at $\sim$ 17.4 keV and $\sim$ 19.6 keV which are considered as the characteristic x-rays of Mo K_α and Mo K_β. These results reveal that more higher energy x-rays from the W x-ray tube are totally reflected on the inner wall of the HfO_2-coated glass monocapillary due to the increase of total reflection critical angle. This work is significant for more applications of monocapillary in higher energy x-ray field.

Keywords: x-ray optics, monocapillary, atomic layer deposition, HfO_2 film

PACS: 07.85.–m, 41.50.+h **DOI:** 10.1088/1674-1056/abcfa2

1. Introduction

Monocapillary, a single hollow tube, is a popular device for x-ray focusing and collimation.[1,2] It usually presents a cylindrical, conically tapered, paraboloidal or elliptical shape[3–5] and is mainly used to obtain a small x-ray beam for experiments such as micro-x-ray fluorescence (micro-XRF) instrument[6,7] and x-ray nano-imaging system.[8,9] In monocapillary, only the portion of x-rays with incident angles less than the critical angle can be totally reflected on the inner wall of the tube and transmitted through the hollow core region. The critical angle for total reflection is determined by the complex index of refraction n,

$$n = 1 - \delta - \mathrm{i}\beta. \tag{1}$$

The theoretical value for δ[10] is

$$\delta = \frac{1}{2} \cdot \frac{e^2}{\pi mc^2} \cdot \frac{N_0 \rho}{A} \cdot Z\lambda^2 = 2.70 \times 10^{10} \times \frac{Z}{A} \rho \lambda^2. \tag{2}$$

In terms of the glancing angle, the critical angle θ_c (rad) can be calculated from the following equation:

$$\theta_c \approx 2.8815 \times 10^{-2} \cdot \sqrt{\frac{Z}{A}\rho} \cdot E^{-1} \quad (\text{assuming } \beta = 0), \tag{3}$$

where Z is the atomic number, A the atomic mass, ρ (in units g/cm^3) the density of the reflective material, and E (in unit keV) the energy of the incident x-rays. It can be inferred that for the same monocapillary the higher the value of E, the smaller the value of θ_c will be.

Due to the easy processing and smoothness of surface, glass is the most common material for both monocapillary[11] and polycapillary.[12] However, the glass density is relatively low (2.2 g/cm^3), which leads to a small θ_c, indicating that part of the high energy incident x-rays emitted from an x-ray tube cannot be totally reflected by the inner wall of the monocapillary. Increasing θ_c is believed to be an efficient way to improve the transmission characteristics by totally reflecting more higher energy x-rays. From this point of view, it can be seen from Eq. (3) that to increase the value of θ_c high-density material is an ideal choice for the capillaries. That is why the metal monocapillaries have received wide attention since 1996. Several methods have been developed to produce 'segmented' and 'pressed' metal monocapillaries. Nevertheless, the shapes of those monocapillaries are far from the design because of narrow etching grooves[10] and horizontal

*Project supported by the National Key Research and Development Program of China (Grant No. 2018YFF0109100), Fund from the Institute of Electrical Engineering, Chinese Academy of Sciences (Grant No. E1554404), and the National Natural Science Foundation of China (Grant Nos. 11675019 and 11875087).

†These authors contributed equally to this work.
‡Corresponding author. E-mail: slkongxd@mail.iee.ac.cn

© 2021 Chinese Physical Society and IOP Publishing Ltd

wedges[13] respectively. Although the process of manufacturing 'segmented' monocapillaries is further optimized[14,15] and monocapillaries with precise shape can be obtained, the smoothness of inner surface can still not be well controlled. Therefore another idea is proposed. That is to coat a high-density film in the inside of capillary and many researchers have tried this method. In 2005 Matsuura *et al.*[2,16] fabricated nickel-coated monocapillaries by a plating method. In order to achieve better adhesion of the nickel layer onto the glass, the surface of the silica was sensitized with ammonium fluoride solution, which resulted in some clusters of nickel on the surface. In 2010 Nakazawa and Nakano[17] used the same method to gain Au-coated monocapillaries and observed the enhancement of XRF intensity, which implies the performance improvement of metal-coated monocapillaries. Unfortunately, owing to the extremely high length–diameter ratio of the capillary, it is still difficult to obtain thin film with uniform thickness and low roughness.

Atomic layer deposition (ALD) is a vapor phase deposition technique based on the sequential use of self-limiting chemical reactions, which ensures the conformality, uniformity and atomic level control of film. Compared with other vapor phase thin film growth methods such as chemical vapor deposition (CVD) or physical vapor deposition (PVD), the ALD due to the self-limiting growth, can be used to deposit a highly homogeneous thin film on the surface of curved substrate without additional manipulation such as rotating the substrate. Until now a variety of films have been successfully deposited by the ALD on many types of substrates such as Si wafers,[18,19] Si nanowires,[20] and glass fiber cores.[21,22] Therefore the ALD is a promising way to coat capillary. And through optimizing the process and improving the equipment, the ALD presents potential applications in coating polycapillary with a diameter less than 10 μm or coating multilayer-film on the inner surface of capillary which is an important x-ray monochromic component. That is of great significance for applying capillaries to more x-ray fields. Our previous work[23] demonstrated that the ALD is a feasible way to coat glass monocapillary with a short length of 5 cm and the coated monocapillary shows an increased acceptance angle for 16.8-keV x-ray while high reflectivity is still retained. Here in this work, the ALD is used to deposit HfO_2 film on the inner surface of monocapillary which is nearly twice as long as the former one, and possesses a higher length-diameter ratio. Based on the working principle, it is known that generally high-density-film coated glass monocapillary with a higher length-diameter ratio will totally reflect more high-energy x-rays if space allows. And monocapillary with length ∼10 cm is commonly used.[2,16,17] The HfO_2 film is selected considering the fact that its density is higher than that of glass and it is chemically stable with melting temperatures as high as 2758 °C. The transmission process of x-ray with energy from 5 keV to 100 keV through the HfO_2-coated monocapillary is analyzed in detail. The HfO_2-coated monocapillary is used in an XRF system and spectrum of a Mo sample is measured.

2. Experiments

2.1. Coating

A tapered borosilicate glass monocapillary was drawn and used to grow HfO_2 film on the inner wall. The length (L), input diameter (ID), and output diameter (OD) of the monocapillary are listed in Table 1. And the monocapillary was designed to focus x-rays by single total reflection. The HfO_2 film was deposited using a commercial Ke-Micro T-ALD 100A setup. The ALD was performed using sequential exposures of TDMAH ($Hf(N(CH_3)_2)_4$) and H_2O separated by a purge of nitrogen with a flow rate of 14 standard cubic centimeters per minute (sccm). The deposition cycle for HfO_2 consisted of 0.13-s pulse of TDMAH, 50 s of purging with nitrogen followed by 0.02-s pulse of H_2O and 50 s of purging with nitrogen. The 3000 ALD cycles were set to deposit on the inner wall of glass monocapillary. The typical growth rate for HfO_2 coating is 0.95 Å per cycle. The deposition temperature and pressure were 250 °C and 0.1 Torr (1 Torr = 1.33322×10^2 Pa) respectively. Scanning electron microscope (SEM) was utilized to observe the cross-section of the HfO_2-coated monocapillary.

Table 1. Parameters of tapered monocapillary.

L (cm)	ID (μm)	OD (μm)	Slope (μrad)
9.9	596.4	402.3	980.3

2.2. Measurement

The spectra of x-rays focused by the tapered monocapillary before and after coating were measured. Figure 1(a) shows the measurement system consisting of an x-ray tube, a beamstop (a lead round ball with diameter ∼ 300 μm), a monocapillary, a Pb plate, and an x-ray detector. The x-ray tube with a W target (L9631 HAMAMATSU, Japan) was operated at 10 W (100 kV, 100 μA) and the size of the x-ray source was ∼21 μm. The beamstop was used to block the direct x-rays. A Pb plate with about 1-mm-diameter pinhole aligning to the exit of the monocapillary could effectively shield the primary x-rays from the source and 'penetration halo' x-rays.[24] A high energy x-ray detector (X-123 CdTe AMETEK, USA) was used to obtain the spectra. F was set to be 20 cm. The detecting time was 5 min.

The spactra of XRF were detected by using the uncoated and HfO_2-coated monocapillarie. Figure 1(b) presents the measurement system. The x-ray tube was operated at 10 W (50 kV, 200 μA). The beam-stop was used to block the direct

x-rays for avoiding the influence of the direct x-rays on the results of XRF. A Mo sample was used and a silicon drift detector system (AXAS-M KETEK, Germany) was utilized to collect the XRF spectrum. The value of F, D, and σ were fixed at 20 cm, 10 cm, and 45° respectively. The detecting time was 10 min.

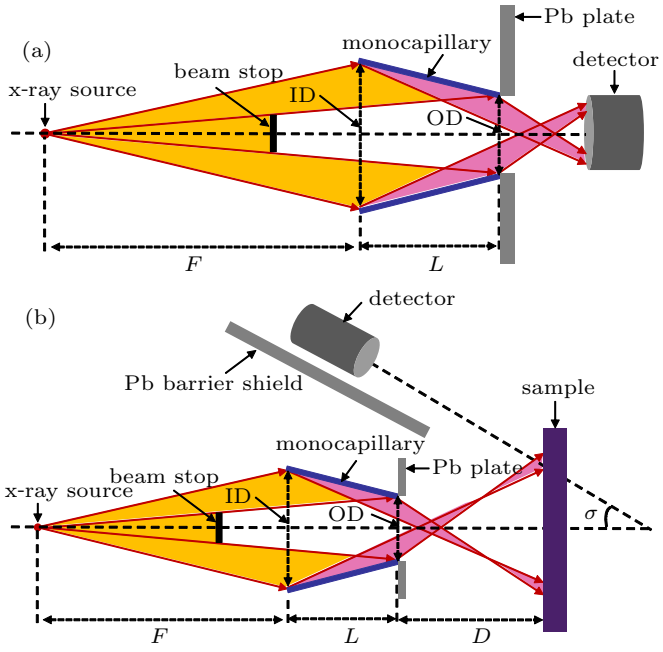


Fig. 1. Sketch of measurement system of spectra of (a) x-rays and (b) XRF by using monocapillary.

3. Results and discussion

3.1. Transmission of x-rays

Figure 2 shows the primary spectrum of the x-ray tube (through a pinhole) and the spectra of x-rays through monocapillary before and after coating. The normalized energy spectrum is obtained through dividing the counts by the highest count of the spectrum. In area 1 the spectrum of x-rays focused by uncoated monocapillary (blue curve) falls rapidly from the blue point at 13.3 keV to the bottom 18.1 keV and that focused by HfO_2-coated monocapillary (red curve) falls from red point at 18.7 keV to the bottom 33.0 keV. Therefore, it can be seen that the energy range of x-rays focused by HfO_2-coated monocapillary is broadened obviously. Figure 3 helps to further understand the propagation of x-rays in the monocapillary. Reflex angle of the incident x-rays reflected by inner surface of the monocapillary goes from θ to θ'. The value of θ, which depends on F, L, ID, and OD, determines the highest energy of x-ray that can be totally reflected on the entire inner surface of the monocapillary. And the value of θ' determines the highest energy of x-ray the monocapillary can focus. According to Eq. (3), for the glass monocapillary before being coated in this work, the highest energy of x-ray reflected on the entire inner surface of the monocapillary is calculated to be 12.1 keV and the highest energy the monocapillary can focus is 17.8 keV, which is basically consistent with the blue curve in area 1 in Fig. 2. Hence the high energy x-rays in a range between 13.3 keV and 18.1 keV can be completely reflected on the inner surface. However, as the energy goes up in this range, the reflective area of the inner surface decreases, which results in the decreasing of x-ray intensity from 13.3 keV and 18.1 keV presented in the spectrum (blue curve). As for HfO_2-coated monocapillary, due to the increase of total reflection critical angle, the energy range of x-rays which can be reflected obviously shifts towards high energy region. Theoretically the highest energy of x-ray reflected on the entire inner surface of the HfO_2-coated monocapillary is calculated to be 23.0 keV and the highest energy the monocapillary can focus is 33.8 keV. In Fig. 2, it is not difficult to find that the red curve between 18.7 keV and 33.0 keV includes two pieces of slopes separated at 23.3 keV. Considering the fact that the density of the HfO_2 film is generally less than 9.85 g/cm^3, the theoretically calculated energy range from 23.0 keV to 33.8 keV is basically consistent with the second slope range from 23.3 keV and 33.0 keV. Nevertheless, why the peak appears at 18.7 keV is not known exactly. Maybe it results from the non uniform distribution of HfO_2 film along the monocapillary and it makes the transmission process of x-rays more complicated. For example, the thicker film on the inner wall of the monocapillary may be right in the path of some totally reflected x-rays and the x-rays have to pass through the film, thereby lead the transmission efficiency and x-ray intensity to decrease.

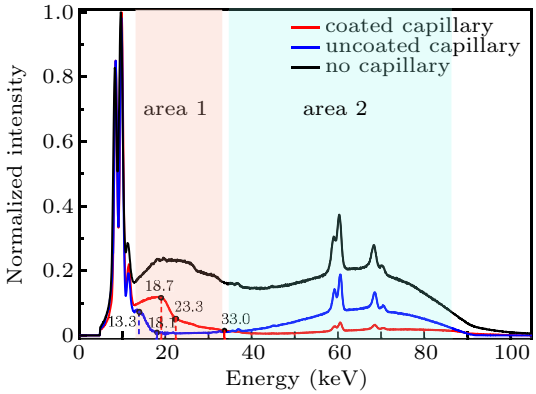


Fig. 2. Primary spectrum of x-ray tube, x-rays through HfO_2-coated monocapillary and uncoated monocapillary, with area 1 and area 2 indicating relatively low and high energy regions respectively.

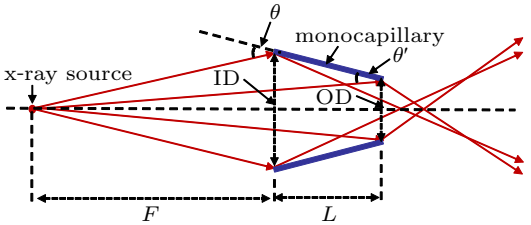


Fig. 3. Sketch of reflection of incident x-rays on inner surface of monocapillary, where θ and θ' are incident angles of x-rays at entrance and exit of monocapillary.

In addition, in area 2 the spectrum of x-rays through uncoated monocapillary goes up at 35 keV and it has the same

trend as the primary spectrum after 35 keV. That is mainly attributed to the effect of 'penetration halo' which results from the high energy x-rays penetrating through the wall of monocapillary and being detected by the x-ray detector. Therefore some x-rays with energy > 35 keV passing through the uncoated monocapillary leads the intensity in the high energy range to increase. At the same time, it can be seen that the spectrum of the HfO_2-coated monocapillary presents no significant increase in that range. Based on that, it could be inferred that high-density HfO_2 film absorbs more high energy x-rays and less x-rays leak outside the monocapillary. And the 'penetration halo' is suppressed to some extent.

3.2. XRF spectrum

Figure 4 shows the XRF spectrum of the Mo sample obtained by using uncoated (green curve) and HfO_2-coated (red curve) monocapillary. The normalized energy spectrum is acquired through dividing the counts by the highest count of the spectrum. In Fig. 4, it can be seen that the two spectra present many peaks, which is because the Mo sample contains a variety of impurity elements. As it is known that only the x-rays with energy higher than the absorption edge of some element can go through monocapillary, the characteristic peaks can appear on the spectrum. The two spectra present peaks at the same positions in the range with x-ray energy < 15 keV, which means that the uncoated and coated monocapillary both can focus x-rays whose energy is high enough to excite these characteristic peaks. However, the key difference between the two spectra is that two more peaks occur at ~ 17.4 keV and ~ 19.6 keV on the red curve. Considering the influence of the energy resolution of the detector, these two peaks are regarded as the characteristic x-rays of Mo K_α (17.48 keV) and K_β (19.606 keV).[25] To excite these two characteristic x-rays of Mo, the energy of the incident x-ray on the sample must be higher than the absorption edge of Mo (20.0 keV). From the analysis in Subsection 3.1, the highest energy the uncoated monocapillary can focus is 18.1 keV, which leads no K-series characteristic x-rays of Mo to appear on the green curve. The highest energy the HfO_2-coated monocapillary can focus is 33.0 keV and hence two strong peaks occur on the red curve. Therefore the ability of HfO_2-coated monocapillary to focus more higher energy x-rays can help to improve XRF measurement.

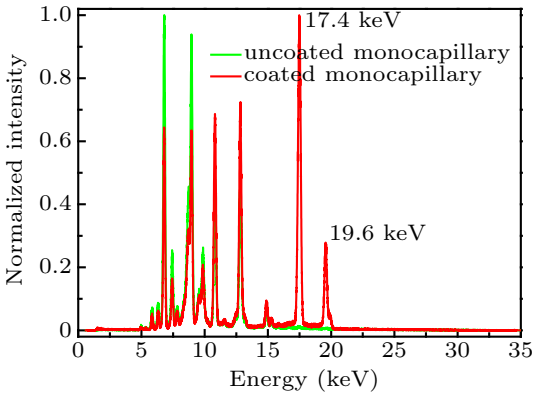


Fig. 4. Sspectrum of XRF obtained by uncoated monocapillary and HfO_2-coated monocapillary.

3.3. HfO_2 film

Figure 5 shows SEM images of the cross-section of HfO_2-coated monocapillary in the middle area. The close up and overall view of monocapillary center hole are presented in the left image and the right image. The thickness of HfO_2 film is ~ 150 nm. In addition, film thickness values at other two positions, ~ 2 cm from input/output end of the monocapillary, are presented in Fig. 6 and they are both ~ 200 nm. It can be seen that the film thickness varies along the monocapillary and the specific thickness distribution needs to be further investigated in future. The thickness is less than 300 nm which is the theoretical value of the HfO_2 film considering the fact that the typical growth rate of HfO_2 on a flat substrate is about 0.95 Å per cycle. The main reason may be that the ALD setup used in this experiment is a common equipment designed for growing film on flat or regular curved substrates. The high length-to-diameter ratio of the monocapillary makes it difficult to control the growth process. The precursor gases, TDMAH ($Hf(N(CH_3)_2)_4$) and H_2O, may be not uniformly adsorbed to the inner surface during every cycle and non-uniform HfO_2 film forms along the monocapillary.

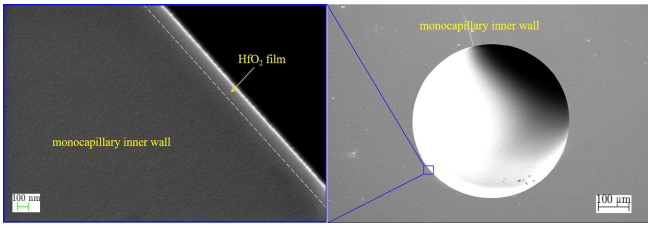


Fig. 5. SEM images of cross-section of HfO_2-coated monocapillary in the middle area.

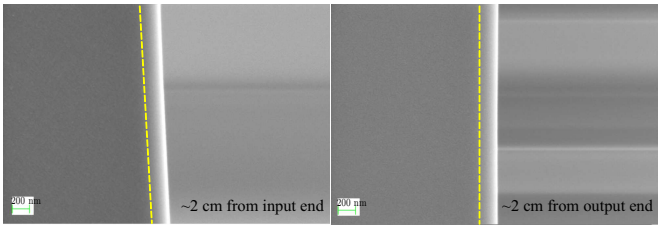


Fig. 6. SEM images of cross-section of HfO_2-coated monocapillary near the two ends.

4. Conclusions and prospects

The results described in this work validate the feasibility of ALD to grow HfO_2 film on the inner wall of larger length-to-diameter ratio monocapillary with length 9.9 cm, entrance diameter 596.4 μm, and exit diameter 402.3 μm. And the HfO_2-coated monocapillary shows improved properties. The energy upper limit of focused x-rays increases from 18.1 keV

to 33.0 keV and the 'penetration halo' is suppressed to some extent. When the HfO_2-coated monocapillary is used in XRF system, more high energy characteristic x-rays are obtained without changing any parameters of the measurement system. Due to the film growth mechanism, the ALD is a promising method to grow single or multilayer film on the inner surface of monocapillary and even polycapillary, which is of great significance for expanding the application field of capillary x-ray optics. In future, research will focus on the growth of film and more applications of the coated capillary. In order to allow the uniform growth of film in a controlled way, critical components of the ALD setup and the deposition process will need to be redesigned and optimized. And the thickness distribution of the film along the monocapillary and its influence on the transmission process will need to be investigated in detail. Besides, some more high-density films such as Ir and Pt can also be deposited inside the capillary to further explore the transmission properties.

References

[1] Erko A, Idir M, Krist T and Michette A G 2008 *Modern Developments in X-Ray and Neutron Optics* (Berlin: Springer-Verlag) p. 288
[2] Matsuura Y, Oyama T and Miyagi M 2005 *Proc. SPIE* **5691** 9
[3] Mroczka R, Zukocinski G and Kuczumow A 2004 *J. Alloys Compd.* **382** 311
[4] Wang Y B, Zhang X Y, Li Y F, Sun X P, Shao S K, Liu Z G and Sun T X 2019 *Nucl. Instrum. Method A* **934** 36
[5] Chen B Z and Yan Y M 1999 *Chin. Phys. Lett.* **16** 630
[6] Zhu Y, Wang Y B, Sun T X, Sun X P, Zhang X Y, Liu Z G, Li Y F and Zhang F Z 2018 *Appl. Radiat. Isotopes* **137** 172
[7] Yang J, Li Y D, Wang X Y, Zhang X Y and Lin X Y 2017 *Nucl. Instrum. Method B* **401** 25
[8] Jiang B W, Liu Z G, Sun X P, Sun T X, Deng B, Li F Z, Yi L T, Yuan M N, Zhu Y, Zhang F S, Xiao T Q, Wang J and Tai R Z 2017 *Opt. Commun.* **398** 91
[9] Wang Y D, Ren Y Q, Sun T X, Tao F, Deng B and Xiao T Q 2018 *Microsc. Microanal.* **24** (Suppl 2) 282
[10] Hirsch G 2003 *X-ray Spectrom.* **32** 229
[11] Li Y D, Lin X Y, Tan Z Y, Sun T X and Liu Z G 2011 *Chin. Phys. B* **20** 040702
[12] Lin X Y, Wang Z H, Chu X L, Sun T X and Ding X L 2007 *Chin. Phys. Lett.* **24** 3368
[13] Hirsch G 2004 *Synchrotron Radiation Instrumentation: Eighth International Conference* p. 728
[14] Mroczka R, Zukocinski G and Kuczumow A 2005 *J. Alloys Compd.* **401** 108
[15] Mroczka R, Bartosik P, Sawłowicz Z, Skrzypiec K, Falkenberg G, Wójcik J, Żukociński G and Kuczumow A 2008 *Thin Solid Films* **516** 8029
[16] Matsuura Y, Oyama T and Miyagi M 2005 *Appl. Opt.* **44** 6193
[17] Nakazawa T and Nakano K 2011 *Powder Diffr.* **26** 163
[18] Gakis G P, Vahlas C, Vergnes H, Dourdain S, Tison Y, Martinez H, Bour J, Ruch D, Boudouvis A G, Caussat B and Scheid E 2019 *Appl. Surf. Sci.* **492** 245
[19] Gougam A B, Rajab B and Afif A B 2019 *Mat. Sci. Semicond. Proc.* **95** 42
[20] Graniel O, Fedorenko V, Viter R, Iatsunskyi I, Nowaczyk G, Weber M, Załęski K, Jurga S, Smyntyna V, Miele P, Ramanavicius A, Balme S and Bechelany M 2018 *Mat. Sci. Eng. B* **236–237** 139
[21] Mayer M, Grevent C, Szeghalmi A, Knez M, Weigand M, Rehbein S, Schneider G, Baretzky B and Schutz G 2011 *Ultramicroscopy* **111** 1706
[22] Sanli U T, Jiao C, Baluktsian M, Grévent C, Hahn K, Wang Y, Srot V, Richter G, Bykova I, Weigand M, Schütz G and Keskinbora K 2018 *Adv. Sci.* **1800346** 1
[23] Wang Y B, Li Y L, Shao S K, Zhang X Y, Li Y F, Sun X P, Tao F, Deng B and Sun T X 2020 *Opt. Commun.* **464** 125544
[24] Sun T X and Ding X L 2004 *Nucl. Instrum. Method B* **226** 651
[25] Luo L Q, Zhan X C and Li G H 2015 *X-ray Fluorescence Spectrometry* (Beijing: Beijing Chemical Industry Press) p. 271 (in Chinese)